

CONF-961040-5

SAND096-2022 C
SAND--96-2022C

Plasma-Induced-Damage of GaN

R. J. Shul, J. C. Zolper, M. Hagerott Crawford, R. J. Hickman, and R. D. Briggs
Sandia National Laboratories, Albuquerque, New Mexico 87185-0603

S. J. Pearton and J. W. Lee
University of Florida, Gainesville, Florida 32611

R. F. Karlicek, Jr., C. Tran, and M. Schurman
EMCORE Corporation, Somerset, NJ 08873

C. Constantine and C. Barratt
Plasma-Therm Inc., St. Petersburg, Florida 33716

RECEIVED

AUG 15 1996

OSTI

Plasma-induced-damage often degrades the electrical and optical properties of compound semiconductor devices. Despite the fact that the binding energy of GaN is larger than that for more conventional III-V compounds, etch damage is still a concern. Photoluminescence measurements and atomic force microscopy have been used to determine the damage induced in GaN by exposure to both electron cyclotron resonance (ECR) and inductively coupled plasmas (ICP) generated Ar plasmas.

INTRODUCTION

Interest in GaN and related group-III nitride materials continues to grow as demonstrations of blue, green, and UV LEDs and lasers and high temperature electronics are reported. The increase in device fabrication may be attributed to significant advances in material growth, improved contacts, ion implant isolation and doping, and dry etch patterning. The most significant advancement in dry etching may be the application of high-density plasmas to the group-III nitrides. Plasma etching of GaN has been reported using several dry etch techniques including reactive ion etch (RIE), electron cyclotron resonance (ECR), inductively coupled plasmas (ICP), and magnetron reactive ion etch (MRIE) systems. Using RIE, GaN etch rates as high as 650 Å/min have been reported at dc-biases of -400 V.[1-3] Significantly higher etch rates have been reported in high-density plasma etch systems at lower dc-biases than those required in RIE systems. GaN etch rates have been reported at 9000 Å/min to 1.3 μm/min at ≤-275 V dc-bias in an ECR, [4-12] 3500 Å/min at -100 V dc-bias in a MRIE, [13] and 6875 Å/min at -280 V dc-bias in an ICP.[14, 15]

Increasing the ion energy in a plasma etch system typically results in highly anisotropic, high rate etching due to the physical sputter desorption of the etch products. However, bombardment of semiconductor surfaces with energetic ions generated during plasma etching can damage the near surface region and produce lattice damage if the ions energy are greater than the displacement energy of the host atoms. As these energetic ions strike the sample, damage as deep as 100 nm can occur, [16] causing degradation of device performance. This damage can include simple Frenkel pairs consisting of a vacancy and the displaced atom, implanted etch ions, broken bonds, formation of dangling bonds, or deposition. Attempts to minimize the damage by reducing the ion energy below the damage threshold for compound semiconductors (< 40 eV) [17] or by increasing the chemical

DISCLAIMER

**Portions of this document may be illegible
in electronic image products. Images are
produced from the best available original
document.**

component of the etch results in more isotropic profiles, significantly limits minimum dimensions, and reduces the etch rate. It is therefore necessary to develop plasma etch processes which couple high etch rates and anisotropy and sidewall profile control for critical dimension with low-damage for optimum device performance.

Since GaN is more chemically inert than GaAs and has higher binding energies, higher ion energies may be used during the etch with potentially less damage to the material. However, reports of plasma-etch-induced-damage of the group-III nitrides has been limited. Pearton and co-workers have reported plasma-induced-damage results for InN, InGaN, and InAlN in an ECR-generated plasma where the damage increased as a function of ion flux and energy.[18] ICP etching offers an attractive alternative etch technique which may be easier to scale-up than ECR sources, and may be more economical in terms of cost and power requirements. ICP plasmas are formed in a dielectric vessel encircled by an inductive coil into which rf-power is applied. A strong magnetic field is induced in the center of the chamber which generates a high-density plasma due to the circular region of the electric field that exists concentric to the coil. At low pressures (≤ 10 mTorr), the plasma diffuses from the generation region and drifts to the substrate at relatively low ion energy. Thus, ICP etching is expected to produce low damage while achieving high etch rates. In this paper, we report ICP and ECR plasma-induced-damage of GaN using PL measurements as well as etch rate results and root-mean-square (rms) surface roughness for GaN as a function of rf-power and source power. Pure Ar plasmas were used to simulate the ion bombardment conditions created during plasma etching of the group-III nitrides.

EXPERIMENTAL

The GaN samples used in this study were grown by metal organic chemical vapor deposition (MOCVD) on a c-plane sapphire substrate in a multiwafer rotating disk reactor at 1040°C with a 20 nm GaN buffer layer grown at 530°C.[19] The GaN film was approximately 1.8 μm thick. The ECR plasma reactor used in this study was a load-locked Plasma-Therm SLR 770 etch system with a low profile Astex 4400 ECR source in which the upper magnet was operated at 165 A. Energetic ion bombardment was provided by superimposing an rf-bias (13.56 MHz) on the sample. Etch gases were introduced through an annular ring into the chamber just below the quartz window. To minimize field divergence and to optimize plasma uniformity and ion density across the chamber, an external secondary collimating magnet was located on the same plane as the sample and was run at 25 A. The ICP reactor was a load-locked Plasma-Therm SLR 770 etch system with a Plasma-Therm 2 MHz ICP source. The reactor was a cylindrical coil configuration with a dielectric vessel encircled by an inductive coil into which the rf power was applied. Identical to the ECR, energetic ion bombardment was provided by superimposing an rf-bias (13.56 MHz) on the sample. Etch gases were introduced through an annular region at the top of the chamber. Unless otherwise mentioned, ECR and ICP etch parameters used in this study were: 40 sccm of Ar, 30°C electrode temperature, 1 mTorr total pressure, 500 W of applied source power, and 1 to 250 W rf-power with corresponding dc-biases of -10 to -300 ± 25 V.

All samples were mounted using vacuum grease on an anodized Al carrier that was clamped to the cathode and cooled with He gas. Samples used to measure photoluminescence intensity were 5 mm x 5 mm and unpatterned. Samples used to calculate etch rates were patterned using AZ 4330 photoresist. Etch rates were calculated from the depth of etched features measured with a Dektak stylus profilometer after the

photoresist was removed with an acetone spray. Each sample was approximately 1 cm² and depth measurements were taken at a minimum of three positions. Standard deviation of the etch depth across the sample was nominally less than $\pm 10\%$ with run-to-run variation less than $\pm 10\%$. Root-mean square (rms) surface roughness was quantified using a Digital Instruments Dimension 3000 atomic force microscope (AFM) system operating in tapping mode with Si tips.

Photoluminescence (PL) measurements were made at liquid helium temperature (10 K) in a continuous flow cryostat. A HeCd laser (325 nm) was used as the excitation source and the typical excitation power was 5 mW. The detection system consisted of a 0.275 meter spectrometer in conjunction with a thermoelectrically cooled UV-enhanced CCD detector. Measurements were taken using a 1200 line/mm grating for high resolution data and a 150 line/mm grating for low resolution, broad spectral range data. To evaluate the effect of high temperature on the PL, samples were annealed in an Addax AET rapid thermal annealer in flowing argon, preceded by a three cycle pump/purge sequence to reduce the background oxygen level. In the annealer, samples were contained in a SiC coated graphite crucible with thermocouples monitoring the temperature at two points on the crucible. Anneal times were 30 s at the prescribed set point ± 10 °C.

RESULTS AND DISCUSSION

Prior to the etch experiments, the two inch GaN wafer was mapped out to examine the uniformity of the photoluminescence emission. In Figure 1, we show the photoluminescence spectrum at the center of the wafer taken with the low resolution grating. The spectrum consisted of two distinct features. The dominant near band-edge resonance was seen at 3.472 eV (as verified by spectra taken with 1 meV resolution). Emission resonances in this spectral region have been identified with recombination of a neutral-donor-bound exciton [20, 21]. The free exciton resonance, expected at an energy of approximately 3.485 eV [20], was not clearly resolved. The broad spectral feature centered at approximately 2.21 eV was associated with emission from deep level impurities. The oscillations in the deep level emission were due to optical interference effects in the film. We focused on the near-band-edge emission for the majority of our etch studies.

In Figure 2, we plot the peak intensity of the near band-edge emission as a function of radial position on the two inch GaN wafer. The intensity dropped by approximately 15% at a radial position of 0.5 inches and approximately 30 % at a radial position of 0.8 inches. Toward the edge of the wafer, the intensity drop was significantly more rapid. The samples that were used in the etch studies were diced from the center part of the wafer, within the 0.6 inch radial position. The photoluminescence spectra were taken before and after etching for each 5 mm x 5 mm sample. The PL spectrum of a reference sample from the wafer was compared during each experiment to ensure consistency of the excitation conditions. The PL band-edge emission is expected to be accurate to $\pm 5\%$.

The first study evaluated the effect of rf-power on the peak near band-edge PL intensity. GaN samples were exposed to ICP- and ECR-generated Ar plasmas for 1 minute under identical plasma conditions while the rf-power was increased. The dc-bias was approximately 10 to 65% higher in the ECR under comparable conditions. In Figure 3, the percent change in the peak PL intensity versus rf-power is plotted for both ECR and ICP etching. For the ICP case, at relatively low rf-powers (1 and 50 W) the PL intensity slightly degraded, and as the rf-power was increased up to 250 W increasing degradation in PL intensity was seen. Depth profiling of similar films that were patterned under the 1 W (~ 10 V dc-bias) conditions revealed no detectable material removed whereas the 250 W

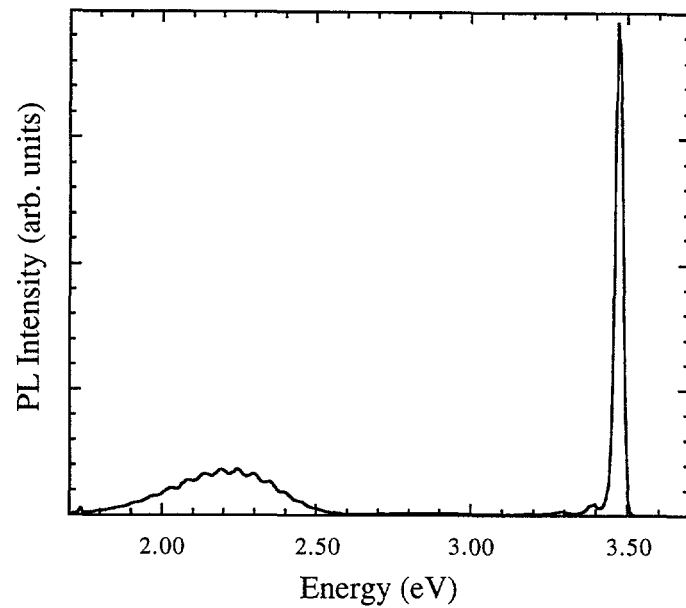


Figure 1: PL spectrum from the GaN film at T=10 K.

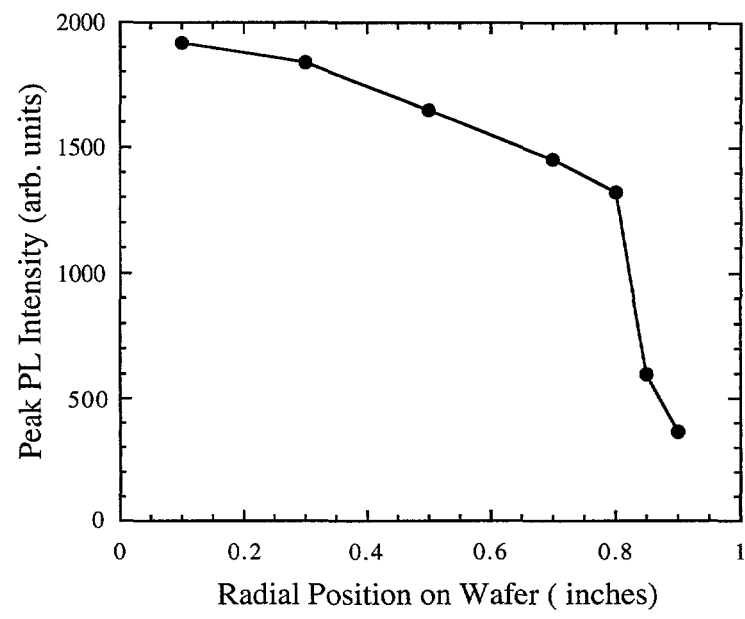


Figure 2: Variation of peak PL intensity as a function of radial position on the two inch wafer

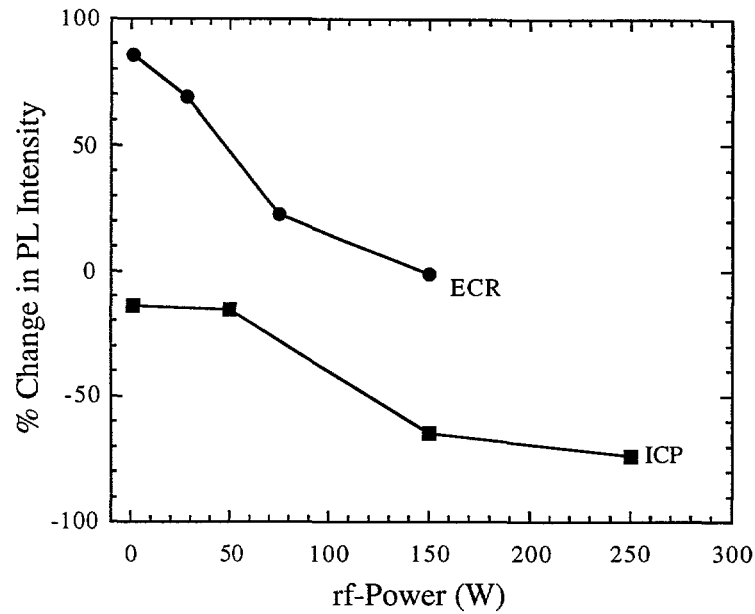


Figure 3: Percent change in the peak PL intensity as a function of rf-power for both ECR and ICP etches.

etch (- 300 V dc-bias) resulted in GaN sputter loss of approximately 770 Å during a 1 minute exposure.

Distinctly different results were obtained for etching in the ECR plasma system. As seen in the figure, etching with very low rf-power (1 W) resulted in an over 80% increase in the photoluminescence intensity. Etching at higher rf- powers also improved the PL intensity, but to a lesser degree as the rf-power was increased. The highest power (150 W) etch resulted in a very slight decrease in PL intensity and the sputter rate under these conditions was determined to be approximately 820 Å/min.

We also studied the effect of plasma density on the peak near band-edge PL intensity. GaN samples were exposed to ICP- and ECR-generated Ar plasmas for 1 minute under identical dc-bias conditions. The dc-bias was held approximately constant at -65 ± 15 V by varying the rf-power. The data was more scattered than the rf-power data for both ICP and ECR conditions. The ICP showed virtually no change in PL intensity at 250 W source power and then decreased by 30% at 750 W. The PL intensity decreased by only 10% at 1000 W ICP power which was an improvement of almost 20% over 750 W. In the ECR, we observed an increase of $\sim 115\%$ in PL intensity at 250 W ECR power. Similar to the trend observed as a function of rf-power, the PL intensity also improved at higher ECR powers but at a lower rate. We did observe an increase of $\sim 250\%$ in PL intensity at 750W ECR power. Sputter rates for GaN ranged from ~ 0 to 225 Å/min as a function of source power in both the ECR and ICP. Further studies are underway to identify the effect of plasma density.

The PL emission efficiency of other III-V bulk semiconductors (e.g. GaAs) has been shown to be strongly dependent on surface conditions, specifically the presence of a native oxide, the surface recombination velocity, as well as band bending at the surface

[22, 23]. Previous work on hydrogen plasma passivation in GaAs films with in-situ PL monitoring has demonstrated that both PL intensity enhancement as well as degradation can occur in different etching regimes. In particular, the reduction of surface As concentration in the initial stages of the etch can result in an increase in the PL efficiency whereas extended exposure to ion bombardment can create damage that reduces the PL efficiency.

While the exact nature of surface oxides and surface states in GaN are not well understood, our data show that the PL efficiency can be strongly affected by exposure to an Ar plasma and is highly sensitive to the exact plasma conditions. A common result for both plasma environments was the decrease in PL intensity with increasing rf-power and source power, which suggested that plasma-induced damage can occur in GaN films under moderate ion energies and plasma densities. Work is in progress to more closely examine the changes in GaN surface conditions under various plasma conditions. Our initial data suggests that GaN surfaces are considerably more sensitive to process-induced changes than is widely recognized. Brief low bias exposures to ECR discharges almost doubled the band-edge PL, suggesting that the native oxide has a strong effect on the surface recombination velocity.

Post-etch anneals in Argon were performed on selected samples to investigate the effects of high temperature on the PL intensity. In Figure 4, we show the change in peak PL intensity as a function of anneal temperature for samples etched under 1 W, 150 W, and 250 W rf-power in the ICP reactor. The post-etch condition, specifically the initial change in PL intensity due to the etch, is indicated as the "no anneal" condition. The data show that the effect of the anneal is strongly dependent on the initial (post-etch) sample conditions. In particular, the sample etched under very low power (1 W) degraded with increasing anneal temperature, whereas the sample etched under moderate power (250 W)

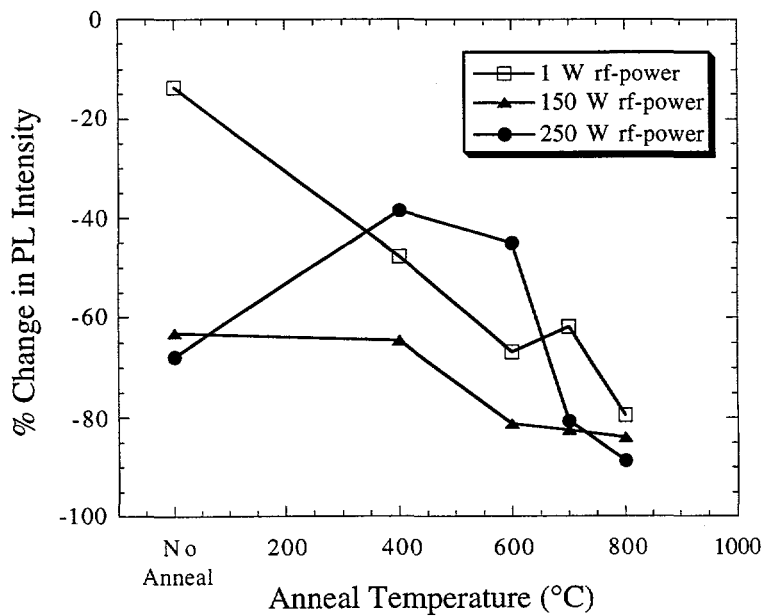


Figure 4: Percent change in the peak PL intensity as a function of post-etch anneal temperature for ICP etched samples. The rf-power etch conditions are indicated in the figure.

showed an initial enhancement in the post-etch PL intensity, followed by degradation as the anneal temperature was increased beyond 400°C. These results suggest that relatively low temperature annealing may reduce the (non-radiative) damage induced under the 250 W etching conditions. In all cases, however, the effect of post-etch annealing in Argon for $T > 700^\circ\text{C}$ resulted in a degradation of the PL intensity. At higher rf-powers we would expect a greater initial PL degradation because of the greater damage depth. The low temperature ($\leq 400^\circ\text{C}$) annealing stage for the 250 W sample may result from the individual damage sites being closer together, as is seen in ion-implanted material, where annealing is actually easier in moderately damaged samples. However the key result is that overall, the etch damage is stable to $> 800^\circ\text{C}$, much higher than in other III-V materials.

Similar post-etch annealing experiments were performed on selected samples etched in the ECR reactor, and the effect on PL intensity is shown in Figure 5. For all rf-power conditions, a degradation in the PL was seen after anneals at 400°C and 800°C. The loss of PL intensity with anneal temperature was similar for all of the samples, in strong contrast to the ICP results. This result was not unexpected, due to the large differences in the PL intensities (post-etch) at the start of the anneal experiments. It is interesting to note that for the highest rf-power conditions, annealing at temperatures as high as 800 °C resulted in a similar reduction of pre-etch PL intensity (75-90%) for both ICP and ECR etches, despite the large discrepancy in post-etch PL intensities.

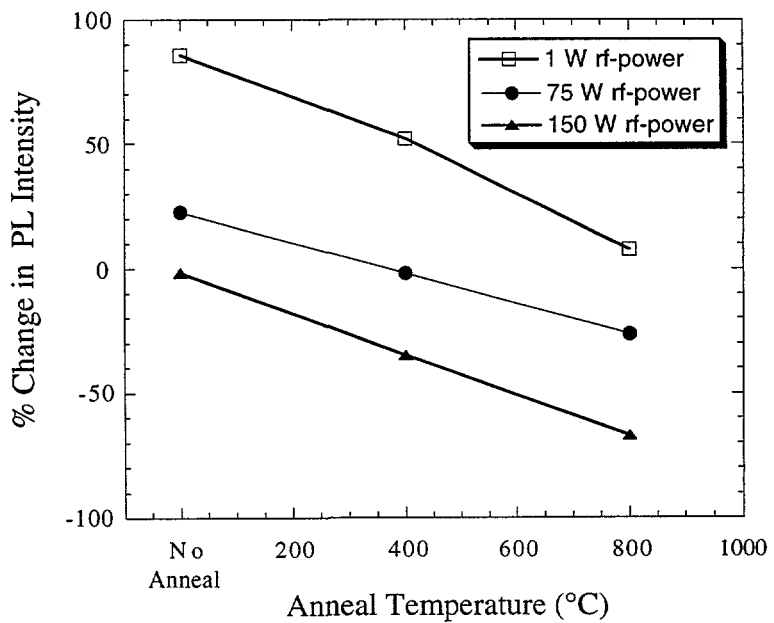


Figure 5: Percent change in the peak PL intensity as a function of post-etch anneal temperature for ECR etched samples. The rf-power etch conditions are indicated in the figure.

Surface roughness was quantified using atomic force microscopy (AFM) to evaluate the effect of the Ar exposure on the root-mean-square (rms) roughness. Samples were measured before and after exposure and showed a slight increase in rms roughness following exposure. In Figure 6, the rms roughness is plotted as a function of rf-power in

an ECR-generated Ar plasma. The post plasma exposure for rms roughness is consistently higher than the as-grown rms roughness, however the difference is a maximum of 1.5 nm which challenges the resolution of the AFM system used. Trends were very similar for rf-power in the ICP and ECR and ICP power. This trend implies that the change in rms surface roughness has little effect on the PL intensity.

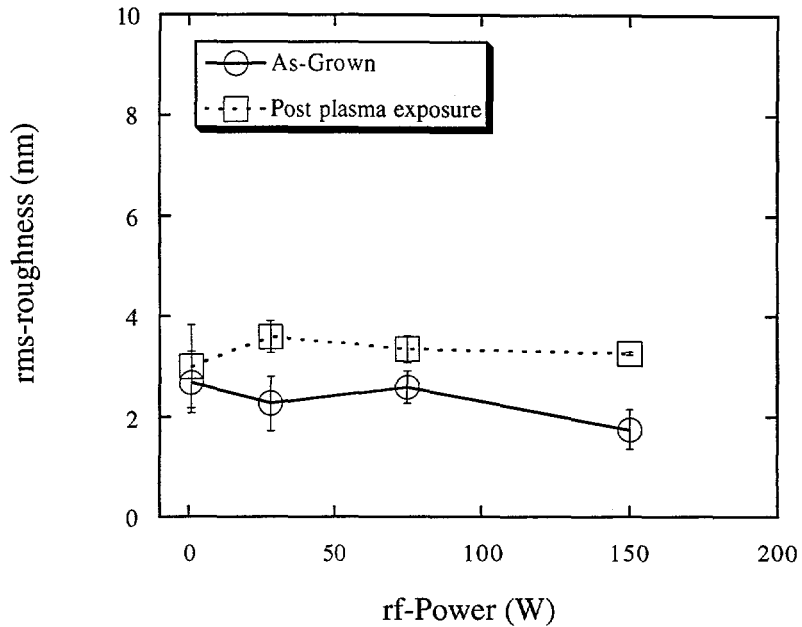


Figure 6: GaN rms surface roughness for as-grown samples and samples exposed to an ECR-generated Ar plasma as a function of rf-power.

It is important to realize that the use of a pure Ar plasma creates a worse case scenario for plasma-induced-damage due to the lack of chemical interactions. With the introduction of reactive gases to the plasma for a given plasma power and density, the damage will be reduced when compared to a sputter mechanism since damaged material is being removed at a given rate, leaving a shallower damage depth. [16, 18] Etch rates for GaN are shown in Figure 7 as a function of rf-power in an ICP and ECR chlorine-based plasma. The etch conditions were; 22.5 sccm Cl₂, 2.5 sccm H₂, 5 sccm Ar, 1 mTorr pressure, 500 W source power, and rf-powers ranging from 1 to 250 W. The GaN etch rates increased monotonically with rf-power independent of etch technique. The ICP etch rates were 10 to 30 % faster than those obtained in the ECR. This trend was observed previously and was attributed to higher concentrations of reactive neutrals formed in the ICP. [14]

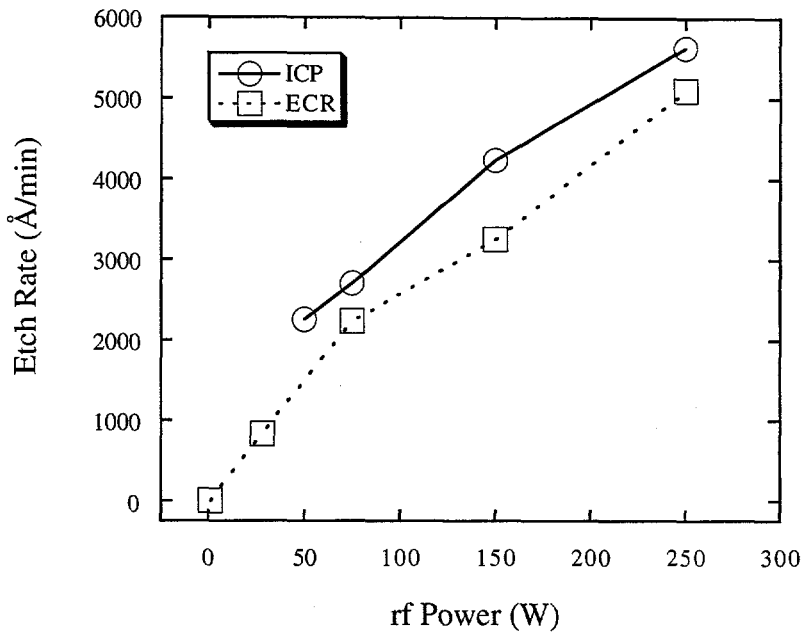


Figure 7: GaN etch rates as a function of rf-power for ICP and ECR $\text{Cl}_2/\text{H}_2/\text{Ar}$ plasmas.

CONCLUSIONS

Peak PL intensity was strongly affected by exposure to an Ar ECR and ICP plasma, with both enhancement and degradation seen under various etch conditions, as is the case with GaAs. For both plasma environments the PL intensity decreased with increasing rf-power and source power. Exposure to an ICP Ar plasma resulted in decreased PL intensity, whereas the PL intensity increased following exposure to the ECR. The effect of post-etch annealing in Ar varies, depending on initial film conditions. For all etch conditions examined in this work, annealing at temperatures above 400°C resulted in a reduction in the PL intensity. Possible degradation mechanisms may be due to defect migration to form stable non-radiative centers, loss of passivating hydrogen initially in the GaN, or the formation of a non-stoichiometric surface oxide. We are currently investigating all of these mechanisms using time-resolved PL and surface recombination velocity measurements. Although the nature of surface states and oxides in GaN is not entirely understood, our results suggest that surface conditions can significantly affect radiative recombination efficiency in GaN films. Further work is in progress to determine the nature and effect of plasma-induced surface passivation in the group-III nitride materials.

ACKNOWLEDGMENTS

The authors would like to thank P. L. Glarborg, and L. Greigo for their technical support. This work was performed at Sandia National Laboratories supported by the U.S. Department of Energy under contract #DE-AC04-94AL85000. The GaN work is partially supported by an DARPA grant monitored by AFOSR (A. F. Witt).

REFERENCES

- [1] I. Adesida, A. Mahajan, E. Andideh, M. Asif Khan, D. T. Olsen, and J. N. Kuznia, *Appl. Phys. Lett.* **63**, 2777.
- [2] M. E. Lin, Z. F. Zan, Z. Ma, L. H. Allen, and H. Morkoc, *Appl. Phys. Lett.* **64**, 887 (1994).
- [3] A. T. Ping, I. Adesida, M. Asif Khan, and J. N. Kuznia, *Electron. Lett.* **30**, 1895 (1994).
- [4] S. J. Pearton, C. R. Abernathy, F. Ren, J. R. Lothian, P. W. Wisk, A. Katz, and C. Constantine, *Semicond. Sci. Technol.* **8**, 310 (1993).
- [5] S. J. Pearton, C. R. Abernathy, and F. Ren, *Appl. Phys. Lett.* **64**, 2294 (1994).
- [6] S. J. Pearton, C. R. Abernathy, and F. Ren, *Appl. Phys. Lett.* **64**, 3643 (1994).
- [9] R. J. Shul, S. P Kilcoyne, M. Hagerott Crawford, J. E. Parmeter, C. B. Vartuli, C. R. Abernathy, and S. J. Pearton, *Appl. Phys. Lett.* **66**, 1761 (1995).
- [10] R. J. Shul, A. J. Howard, S. J. Pearton, C. R. Abernathy, C. B. Vartuli, P. A. Barnes, and M. J. Bozack, *J. Vac. Sci. Technol.* **B13**, 2016 (1995).
- [12] C. B. Vartuli, S. J. Pearton, J. W. Lee, J. Hong, J. D. MacKenzie, C. R. Abernathy, and R. J. Shul, *Appl. Phys. Lett.*, accepted, (1996).
- [13] G. F. McLane, L. Casas, S. J. Pearton, and C. R. Abernathy, *Appl. Phys. Lett.* **66**, 3328 (1995).
- [14] R. J. Shul, G. B. McClellan, S. J. Pearton, C. R. Abernathy, C. Constantine, and C. Barratt, *Electron. Lett.*, submitted, 1996.
- [15] R. J. Shul, G. B. McClellan, S. A. Casalnuovo, D. J. Rieger, S. J. Pearton, C. Constantine, C. Barratt, R. F. Karlicek, Jr., C. Tran, and M. Schurman, *Appl. Phys. Lett.*, accepted, (1996).
- [16] S.W. Pang, *J. Electrochem. Soc.* **133**, 784 (1986).
- [17] C. Constantine, D. Johnson, S.J. Pearton, U. K. Chakrabarti, A.B. Emerson, W.S. Hobson, and A.P. Kinsella, *J. Vac. Sci. Technol.* **B 8**, 596 (1990).
- [18] S. J. Pearton, J. W. Lee, J. D. MacKenzie, C. R. Abernathy, and R. J. Shul, *Appl. Phys. Lett.* **67**, 2329 (1995).
- [19] C. Yuan, T. Salagaj, A. Gurary, P. Zawadzki, C. S. Chern, W. Kroll, R. A. Stall, Y. Li, M. Schurman, C.-Y. Hwang, W. E. Mayo, Y. Lu, S. J. Pearton, S. Krishnankutty, and R. M. Kolbas, *J. Electrochem. Soc.* **142**, L163 (1995).

- [20] W. Shan, T. J. Schmidt, X. H. Yang, J. Hwang, J. J. Song and B. Goldenberg, *Appl. Phys. Lett.* **66**, 985 (1995).
- [21] G. D. Chen, M. Smith, J. Y. Lin, H. X. Jiang, M. Asif Khan and C. J. Sun, *Appl. Phys. Lett.* **67**, 1653 (1995).
- [22] R. A. Gottscho, B. L. Preppernau, S. J. Pearton, A. B. Emerson, and K. P. Giapis, *J. Appl. Phys.* **68**, 440 (1990).
- [23] E. S. Aydil and R. A. Gottscho, *Mat. Sci. For.* 148/149, 159 (1994).

DISCLAIMER

This report was prepared as an account of work sponsored by an agency of the United States Government. Neither the United States Government nor any agency thereof, nor any of their employees, makes any warranty, express or implied, or assumes any legal liability or responsibility for the accuracy, completeness, or usefulness of any information, apparatus, product, or process disclosed, or represents that its use would not infringe privately owned rights. Reference herein to any specific commercial product, process, or service by trade name, trademark, manufacturer, or otherwise does not necessarily constitute or imply its endorsement, recommendation, or favoring by the United States Government or any agency thereof. The views and opinions of authors expressed herein do not necessarily state or reflect those of the United States Government or any agency thereof.
